



# Investigating the Nanocomposite Thin Films of Hematite $\alpha$ -Fe<sub>2</sub>O<sub>3</sub> and Nafion for Cholesterol Biosensing Applications

Indra Sulania<sup>1</sup>, R. Blessy Pricilla<sup>2</sup> and G. B. V. S. Lakshmi<sup>1,3\*</sup>

<sup>1</sup> Materials Science Group, Inter University Accelerator Centre, New Delhi, India, <sup>2</sup> Karunya University, Coimbatore, India, <sup>3</sup> Special Center for Nanoscience, Jawaharlal Nehru University, New Delhi, India

## OPEN ACCESS

### Edited by:

Ajeet Kaushik,  
Florida Polytechnic University,  
United States

### Reviewed by:

Bapu Sumar,  
University of Miami Hospital,  
United States  
Jay Singh,  
Banaras Hindu University, India

### \*Correspondence:

G. B. V. S. Lakshmi  
lakshmigbvs@gmail.com

### Specialty section:

This article was submitted to  
Biomedical Nanotechnology,  
a section of the journal  
Frontiers in Nanotechnology

Received: 21 July 2020

Accepted: 26 October 2020

Published: 26 November 2020

### Citation:

Sulania I, Pricilla RB and  
Lakshmi GBVS (2020) Investigating  
the Nanocomposite Thin Films of  
Hematite  $\alpha$ -Fe<sub>2</sub>O<sub>3</sub> and Nafion for  
Cholesterol Biosensing Applications.  
Front. Nanotechnol. 2:585721.  
doi: 10.3389/fnano.2020.585721

Nanocomposite materials are multi-phase materials, usually solids, which have two or more component materials having different chemical and physical properties. When blended together, a newer material is formed with distinctive properties which make them an eligible candidate for many important applications. In the present study, thin films of nafion (polymer) and hematite or  $\alpha$ -Fe<sub>2</sub>O<sub>3</sub> (nanoparticles) nanocomposite is fabricated on indium tin oxide (ITO) coated glass substrates, due to its enhanced ionic conductivity, for cholesterol biosensor applications. Scanning electron microscopy and Atomic force microscopy revealed the formation of nanorod structured  $\alpha$ -Fe<sub>2</sub>O<sub>3</sub> in the films. The cyclic voltammetry (CV) studies of nafion- $\alpha$ -Fe<sub>2</sub>O<sub>3</sub>/ITO revealed the redox properties of the nanocomposites. The sensing studies were performed on nafion- $\alpha$ -Fe<sub>2</sub>O<sub>3</sub>/CHOX/ITO bioelectrode using differential pulse voltammetry (DPV) at various concentrations of cholesterol. The enzyme immobilization led to the selective detection of cholesterol with a sensitivity of  $64.93 \times 10^{-2} \mu\text{A} (\text{mg/dl})^{-1} \text{cm}^{-2}$ . The enzyme substrate interaction (Michaelis–Menten) constant  $K_m$ , was obtained to be 19 mg/dl.

**Keywords:** cholesterol, iron oxide nanoparticles, electrochemical detection, DPV, biosensor

## INTRODUCTION

Nanocomposite (NC) materials are multiphase solid materials which have one of the blended materials in nano dimensions (Ajayan et al., 2006). The structure of nanocomposites mostly consists of the matrix material which may contain the nano-sized reinforcement components in the form of particles, fibers, nanotubes, etc. Nanocomposites are also found in nature in abalone shell and bone in living beings (Din, 2019). NC are different from the standard composite due to the atypically higher surface to volume percentage of the reinforcing agent and/or higher aspect ratio. Generally, composites are materials made from two or more different materials each having dissimilar physical and chemical properties. The composite materials often exhibit unique characteristics compared to their individual components. Such materials are stronger, lighter, less expensive to prepare (Ajayan et al., 2006; Din, 2019).

Metal oxide nanoparticles have several applications in various fields as electronic, optical, biosensing, catalytic, cosmetic, telecommunication, pharmaceutical areas etc. (Demir et al., 2015). Fe<sub>2</sub>O<sub>3</sub> NPs were used as a chemisorptive to remove the metals from aqueous solutions (Grover et al., 2012). Heavy metal ions such as Cd<sup>2+</sup>, Zn<sup>2+</sup>, Pb<sup>2+</sup>, and Cu<sup>2+</sup> have been successfully

removed from the aqueous solution by the use composite of polymer and magnetic NPs as reported by Ge et al. (2012). Sorption kinetic study was done in the different phases of selenite and selenate by the application of pressurized aged iron oxide nanomaterials (Gonzalez et al., 2012). The catalytic activity of  $\text{Fe}_2\text{O}_3$  NPs in wastewater treatment is extensively used in lab tests too (Perez, 2007). The tendency of  $\text{Fe}_3\text{O}_4$  NPs in oxidation and agglomeration, restricts its usage, therefore, many researchers have encased them in a shell of different material to avoid them from oxidation and agglomeration (Sharma et al., 2013). Specifically, the encasing of oxide nanoparticles with electroactive polymers is useful for application in biosensors as they improve the biocompatibility with the improvement in the ligand exchange between the metal-oxide nanoparticles and biomolecules which is the crucial property for biosensor application (Jun et al., 2008). Nafion is the well-known electroactive polymer, that was used in electrochemical platforms. It was found that, in aqueous solutions, Nafion is used as a proton conductor and it does not mitigate the electrochemical response of the inserted electroactive species therefore used as a binder in the electrocatalytic devices and the phase separation takes place in the ionomer allows the formation of a continuous network of ion conducting channels (Chen et al., 2018). The Nafion/MNPs nanocomposite shows high ionic conductivity (Raymond et al., 1996).

Iron oxide nanoparticles composited with Nafion were used as very good sensors toward glucose and cholesterol (Woo et al., 2003; Umar et al., 2014). It was reported that, the presence of sulphonated groups led to an increase in the absorbed moisture in nafion and  $\alpha\text{-Fe}_2\text{O}_3$  composite. The  $\alpha\text{-Fe}_2\text{O}_3$  nanostructures shows very high density and they have a very good crystallinity due to its rhombohedral structures. The sensors produced can have very good reproducibility with a good detection limit of  $0.018\ \mu\text{M}$  (Hasanabadi et al., 2013). Further, an immobilized enzyme on  $\alpha\text{-Fe}_2\text{O}_3$  may ensure prolonged activity and hence enhanced stability of the biosensors. It has been reported that the activated GOx displayed good catalytic activity toward glucose, and  $\text{Fe}_3\text{O}_4$  nanoparticles provide suitable domain to immobilize GOx and helps in electron transfer among the analyte (glucose) and electrode surface ( $\text{CH-Fe}_3\text{O}_4/\text{ITO}$ ) in the biosensing applications (Kaushik et al., 2008a).

Biosensors have vast applications in various fields such as food and environmental industry, fermentation industry, medical sciences, and plant biology sector along with marine and defense fields (Mehrotra, 2016). Extensive research is going on all around the world to improve the performance, in terms of sensitivity and selectivity, user friendly and to reduce the cost of the biosensors so that it can be available at lower prices to the people. Few of the biosensors work based on iron oxide nanoparticles has been highlighted here. Kaushik et al. (2009) have studied the nano-bio-composite of CH and  $\text{Fe}_3\text{O}_4$  in super-paramagnetic form to detect the urea via immobilization of Urs and GLDH. The biosensor exhibits linearity in the range  $\sim 5\text{--}100\ \text{mg/dL}$  with a weak detection  $\sim 2\ \text{mg/dL}$ . The sensor had a response time of 10 s with sensitivity of  $12.5\ \mu\text{A/mM cm}^{-2}$ . In another work,

surface charged  $\text{Fe}_3\text{O}_4$  NPs comes together and agglomerate in the CH matrix to form bio-composite to detect antigens Ochratoxin A, via immobilizing the IgGs and bovine serum albumin in rabbit. It showed good sensitivity in the order of  $\sim 3.6 \times 10^{-5}\ \text{A dL}^{-1}$ , and has a reproducibility and long-term stability in comparison to CH/ITO based immunosensors (Kaushik et al., 2008b). They have also studied the composite for glucose sensing. The nanocrystals of  $\text{Fe}_3\text{O}_4$  with an average size of 10 nm were synthesized on silica by Sharma et al. (2013). Due to non-conducting nature of  $\text{Fe}_3\text{O}_4/\text{SiO}_2$  NPs, they showed bad response toward electrochemical activities. Further, synthesis of  $\text{Fe}_3\text{O}_4/\text{C}$ , in non-crystalline film, resulted in a good cholesterol biosensor. The Nps showed sensitivity in the order of  $\sim 193$  and  $218\ \text{nA mg}^{-1}\text{dl cm}^{-2}$ , as observed from cyclic voltammetry studies. It was concluded that the encasing  $\text{Fe}_2\text{O}_3$  NPs with conducting polymers like polypyrrole and polyaniline etc., may enhance the sensitivity of biosensor.

The literature survey revealed that, cholesterol sensing can be done using various metal oxide-chitosan composites and some work was performed in the field of nanocomposite bio-sensors using iron oxide nanoparticles synthesized by various other methods for the detection of few analytes. Whereas, iron oxide nanoparticles for biosensing of cholesterol was not reported. This has motivated us to carry-out this study and synthesize a nanocomposite material to sense cholesterol in a user-friendly way. In the present study, we have synthesized nafion-iron oxide nanocomposites and tested for cholesterol sensing applications with and without cholesterol oxidase enzyme (CHOx) enzyme. The composites show good sensitivity with and without the help of CHOx enzyme, whereas the selectivity was obtained only after the immobilization of enzyme. The enzyme CHOx was immobilized on the electrodes without the help of any cross-linking agent. The electrodes showed a very good sensitivity of  $64.93 \times 10^{-2}\ \mu\text{A (mg/dl)}^{-1}\ \text{cm}^{-2}$  for with enzyme and  $0.012\ \text{mA (mg/dl)}^{-1}\ \text{cm}^{-2}$  for without enzyme in the detection range of  $0\text{--}390\ \text{mg/dl}$ . The enzyme—substrate kinetic parameter was obtained to be  $19\ \text{mg/dl}$  which is very less indicating the indicates increased affinity of nafion- $\alpha\text{-Fe}_2\text{O}_3/\text{CHOx}/\text{ITO}$  bioelectrode that is attributed to favorable conformation of ChOx and higher loading onto the electrode. The composite prepared by very simple method in the present work which showed higher sensitivity and better selectivity.

## EXPERIMENTAL

### Reagents

Nafion (Sigma),  $\alpha\text{-Fe}_2\text{O}_3$  (Merck), Cholesterol (Sigma), Phosphate buffer solution (prepared using monosodium and disodium phosphate salts, in the lab), ferri and ferrocyanide (Sigma-Aldrich), Indium Tin Oxide (ITO) coated glass substrates, Cholesterol oxidase (Sigma), Alcohol, acetone and de-ionized water.

### Instruments

A composite film of Nafion/ $\alpha\text{-Fe}_2\text{O}_3$  films deposited on ITO glass substrates were characterized by D8 X-ray diffractometer

(with x-ray source of  $\text{CuK}\alpha$  at 1.54 Å wavelength) from Bruker. The functional group study was carried out using Fourier transform infrared spectroscopy (FTIR) on Bruker model Tensor 37 FTIR spectrometer. The morphology of the composite films was observed using 25 keV electron beam in field emission scanning electron microscope (FESEM) from MIRA II LMH (TESCAN). The films were further characterized with Nanoscope IIIa Atomic Force Microscope (AFM) for the topological studies (Sulania et al., 2018). The contact angle measurements with water drop were performed using DSA3 contact angle measurement set-up from KRUSS. In bulk materials and polymers, the dynamics of the water droplet mostly hinge on the liquid-surface interaction. The curvature of the droplet varies when the water droplet falls on the surface of the thin film showing the interaction between them (Bico et al., 2002). A 3-electrode electro-chemical cell assembly was used for the Electrochemical studies with Pt wire as the counter electrode (CE), nafion- $\alpha\text{-Fe}_2\text{O}_3/\text{ITO}$  as the working electrode (WE) and Ag/AgCl as the reference electrode (RE) dipped into the solution of PBS (0.1M PBS, pH 7.4) comprising 5 mM  $[\text{Fe}(\text{CN})_6]^{3-/4-}$  and the redox probe allied to CHI-600D electrochemical analyzer. Further, the Cyclic Voltammetry studies were performed to observe the redox behavior of the nafion- $\alpha\text{-Fe}_2\text{O}_3/\text{ITO}$  electrodes. The sensing measurements were performed on nafion- $\alpha\text{-Fe}_2\text{O}_3/\text{ITO}$  and nafion- $\alpha\text{-Fe}_2\text{O}_3\text{-CHOx}/\text{ITO}$  electrodes with change in concentration of the cholesterol using electrochemical differential pulse voltammetry method.

### Electrode Preparation

In the present work, thin films of nanocomposite of  $\alpha\text{-Fe}_2\text{O}_3$  nanoparticles with nafion polymer have been fabricated after forming a uniform solution (as shown in **Figure 1**) by solution mixing method and then drop casting the films of this composite onto the ITO substrates. Nafion is a synthetic polymer. It is a tetrafluoroethylene-based fluoropolymer—copolymer. It has excellent thermal and mechanical stability. Its unique ionic properties arise due to the presence of sulfonate groups. The chemical formula of nafion is  $\text{C}_7\text{HF}_{13}\text{O}_5\text{S}\cdot\text{C}_2\text{F}_4$ . Nafion functions as an ion exchange resin and acid catalyst because of the strong acidic properties of the sulfonic acid group.

Iron oxide ( $\text{Fe}_2\text{O}_3$ ) or Ferric oxide is the main source of iron in the steel industry. It is ferromagnetic in nature, commonly known as rust and in chemical terms it is known as hydrated ferric oxide. It exists in three phases; Alpha phase, Gamma phase and Beta phase. The most stable one is the alpha phase (Sulania et al., 2016). The nanoparticles of  $\alpha\text{-Fe}_2\text{O}_3$  exhibit super para magnetism and show low toxicity. They are biocompatible and may be used as a distinction agent in magnetic resonance imaging and as guided carriers in drug discovery. They exhibit long term chemical stability in neutral solution. They are also used as catalyst and photocatalyst.  $\alpha\text{-Fe}_2\text{O}_3$  nanostructures have good stability under physiological conditions. Therefore, we intended to form the composite of the nafion and iron oxide as iron oxide nanoparticles to improve the ionic exchange interaction



**FIGURE 1** | Nano-composite solution of nafion- $\alpha\text{-Fe}_2\text{O}_3$ .

when composited with the polymeric chains of nafion during the sensing of cholesterol.

## RESULTS AND DISCUSSIONS

### Morphology Studies (SEM and AFM)

The surface morphology of  $\alpha\text{-Fe}_2\text{O}_3$ -nafion nanocomposite films formed on ITO was observed using FESEM and AFM. SEM analysis confirms the rod type structure of the  $\alpha\text{-Fe}_2\text{O}_3$  nanoparticles and the images are shown in **Figures 2a,b**. A thin layer covering the rod type structures is observed at higher magnification image in **Figure 2b** showing nafion was surrounding the nanoparticles in the composite. The diameter of the rods is  $<50$  nm including the nafion coating. The EDX analysis carried out on  $\alpha\text{-Fe}_2\text{O}_3$ -nafion nanocomposite films during FESEM study showed the presence of the elements Fe, O, S, F, and C as shown in the **Figure 2c**, which is clearly indicating the formation of the nanocomposite.

**Figure 3** shows the 2D, 3D AFM images of  $\alpha\text{-Fe}_2\text{O}_3$ -nafion nanocomposite film and the sectional analysis of the single rod. These AFM images clearly indicate the rod like structures that were observed in SEM images also. The breadth of a rod has been calculated using section analysis. The horizontal diameter of the rods is found to be 33 nm which is in agreement with the diameter of the rods  $<50$  nm that was observed in SEM images.

### XRD and FTIR Studies

The composite films deposited on glass substrates were used for XRD measurements. XRD spectrum was carried out in the

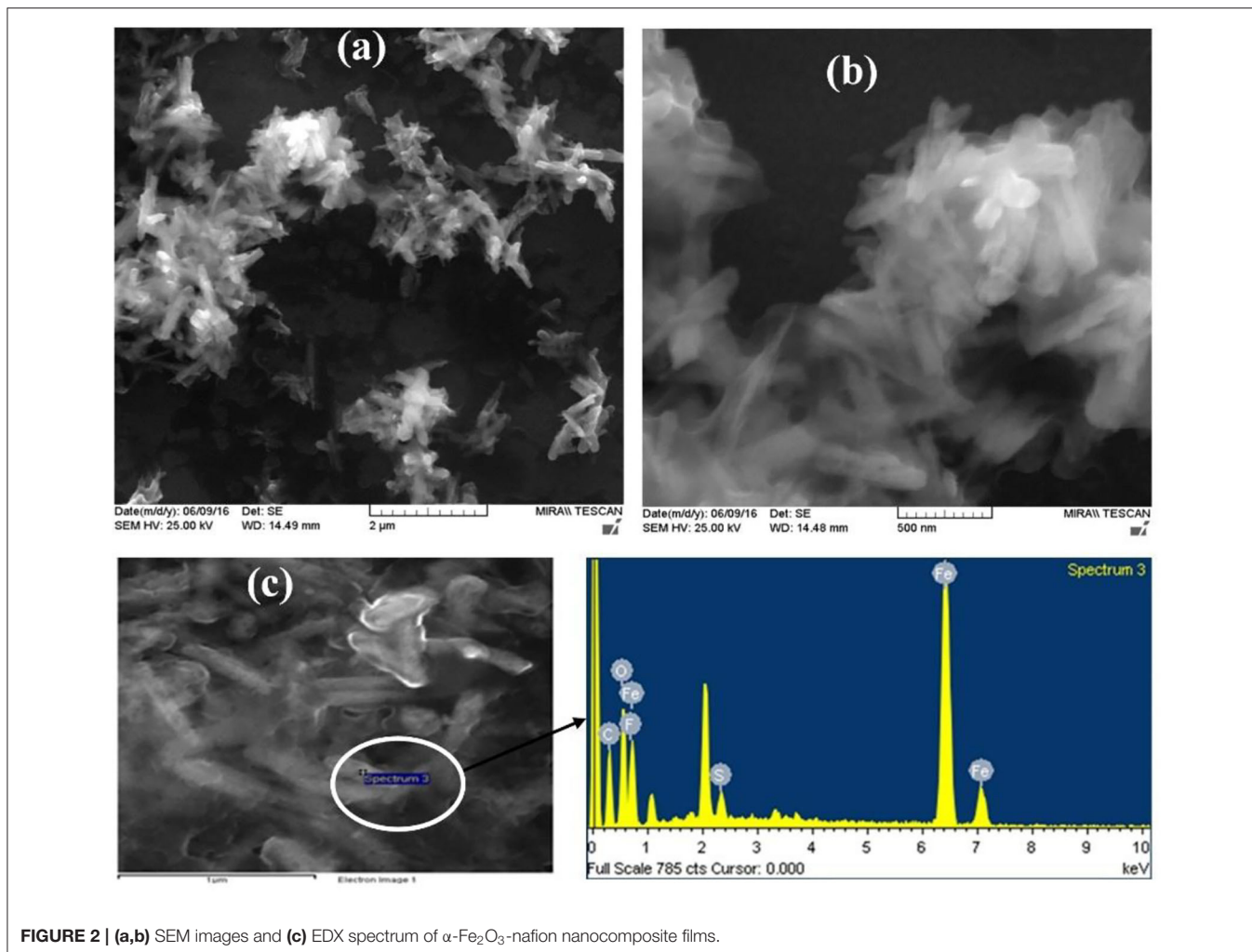


FIGURE 2 | (a,b) SEM images and (c) EDX spectrum of  $\alpha$ -Fe<sub>2</sub>O<sub>3</sub>-nafion nanocomposite films.

range of  $2\theta$  from  $10^\circ$  to  $50^\circ$  using Cu-K $\alpha$  source with wavelength  $1.54\text{\AA}$  with scan rate  $1^\circ$  per sec and the spectrum was shown in **Figure 4A**. The peaks visible at  $2\theta \approx 21.8^\circ(111)$ ,  $27.5^\circ(012)$ ,  $30.1^\circ(220)$ ,  $35^\circ(104)$ ,  $43^\circ(113)$ , confirms the formation of  $\alpha$ -Fe<sub>2</sub>O<sub>3</sub> phase in the composite film (Banerjee et al., 2011; Mallick and Dash, 2013).

From the Scherrer's formula the crystallite size can be estimated as:

$$\beta \cos(\theta) = \frac{K\lambda}{D}$$

where  $K = 0.98$ ,  $D$  is the crystallite size,  $b$  is the FWHM of the highest intense peak and  $l$  is the incident x-ray wavelength. The crystallite size was obtained as  $33.8\text{ nm}$  for the highest intense peak corresponding to (220).

**Figure 4B** shows the FTIR spectra of nafion- $\alpha$ -Fe<sub>2</sub>O<sub>3</sub>/ITO (a) and nafion- $\alpha$ -Fe<sub>2</sub>O<sub>3</sub>/CHOx/ ITO (b) electrodes. The peaks at  $440$  and  $520\text{ cm}^{-1}$  were attributed to Fe-O bond vibrations. The peaks at  $985$ ,  $1,065$ ,  $1,155$ ,  $1,227$ ,  $1,285\text{ cm}^{-1}$  correspond to S-O, C-O-C, C-F, and SO<sub>3</sub>H in sulfonic acids, C-F stretch bands

respectively of nafion. The peak at  $1,650\text{ cm}^{-1}$  corresponding to C=O was observed in the enzyme electrode spectrum (b). The major changes observed in the peaks at  $1,065\text{ cm}^{-1}$  after the enzyme incorporation and appearance of peak at  $1,650\text{ cm}^{-1}$  confirming the successful immobilization (Chen et al., 2013; Singh et al., 2016). The functional groups on nafion helped in the immobilization of CHOx on the electrode.

## Water Wettability Studies

It is well-known that nafion is a super hydrophobic polymer and therefore not useful for sensing. Whereas, when nafion is used in composite form, the properties such as hydrophobicity, photon conductivity, water swelling properties etc. of the composite films found much more different than their individual components (Paul and Karan, 2014; Paul et al., 2016; Kurihara et al., 2017; Singh et al., 2019). The composite films were formed on the ITO coated glass plates and CHOx enzyme was immobilized on one electrode. The contact angle of the composite films before (a) and



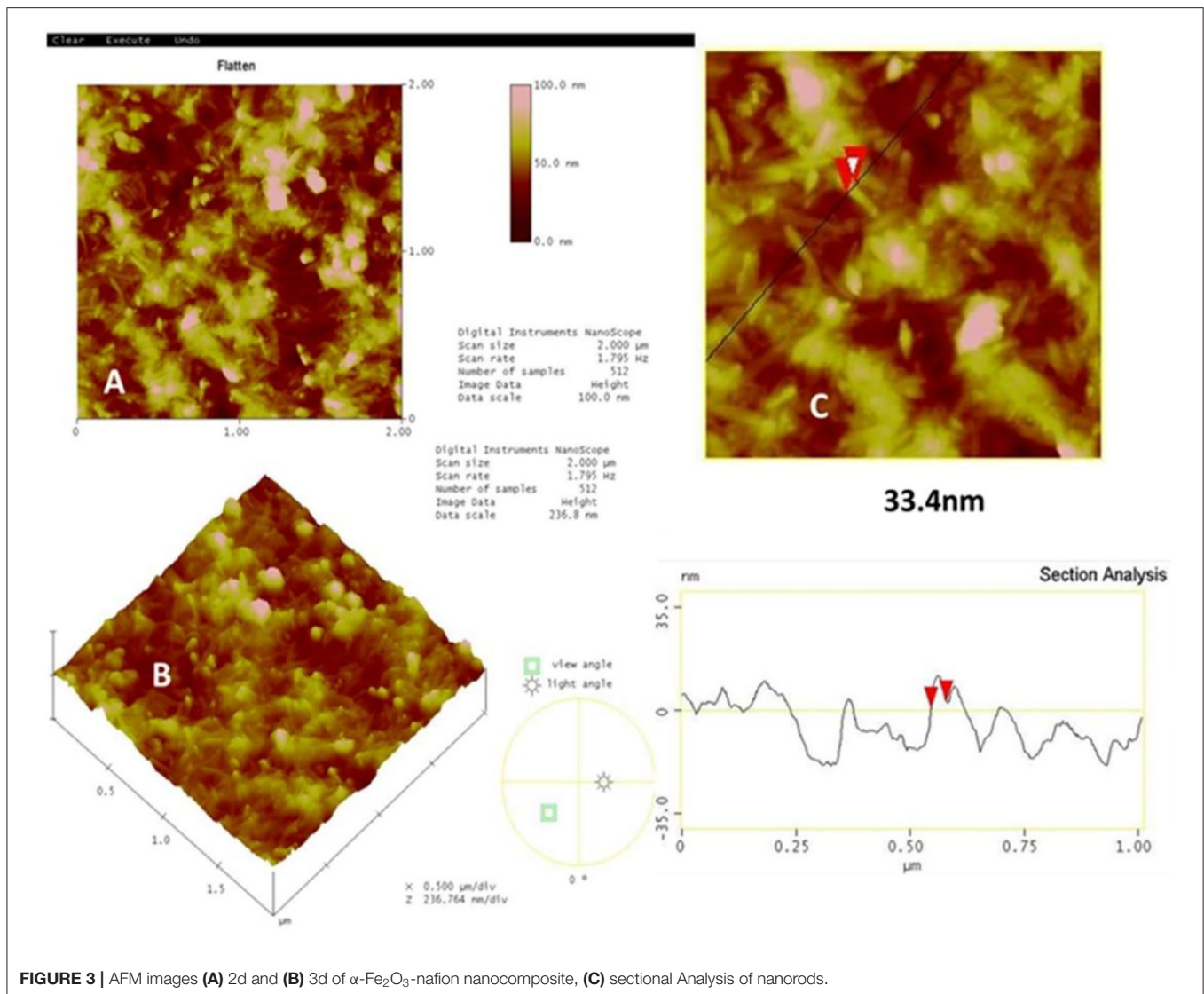


**FIGURE 3** | AFM images (A) 2d and (B) 3d of  $\alpha$ -Fe<sub>2</sub>O<sub>3</sub>-nafion nanocomposite, (C) sectional Analysis of nanorods.

after enzyme immobilization (b) of CHOx on the nanocomposite films are shown in **Figure 5**.

It was found that the contact angle was  $98.64^\circ \pm 2.7^\circ$  of the  $\alpha$ -Fe<sub>2</sub>O<sub>3</sub>-nafion-nanocomposite films showing slightly hydrophobic nature due to the presence of nafion. Upon the immobilization of the enzyme CHOx, the contact angle was drastically reduced to  $8.05^\circ \pm 1.46^\circ$ . So, the films have become completely hydrophilic in nature, which is the foremost requirement for the biosensing applications. The contact angle changed due to the incorporation of nanoparticles that were present in the nanocomposite that modified the surface as of only nafion. Further, enzyme immobilization led to increase in water surface interaction which contributed to the decrease in CA (Singh et al., 2019).

## Electrochemical Studies

The electrochemical properties of nafion- $\alpha$ -Fe<sub>2</sub>O<sub>3</sub>/ITO and nafion- $\alpha$ -Fe<sub>2</sub>O<sub>3</sub>/CHOx/ITO electrodes were studied by CV

technique in a three-electrode cell of 7.4 pH PBS buffer solution comprising 5 mM [Fe(CN)<sub>6</sub>]<sup>3- / 4-</sup> used as the redox species. The CV curves of nafion- $\alpha$ -Fe<sub>2</sub>O<sub>3</sub>/ITO and nafion- $\alpha$ -Fe<sub>2</sub>O<sub>3</sub>/CHOx/ITO obtained at various scan rates shown in **Figures 6A,B**, respectively.

**Figure 6** shows the good oxidation and reduction peaks for both the nanocomposite films. The increase in current with the increase in the scan rate shows the favorable redox nature of the electrodes for electrochemical sensing applications. The anodic and cathodic peak currents and the area of the CV curve were found to increase with scan rate. This increase implies the homogeneous electron transfer of the electrodes. The plot between scan rate<sup>1/2</sup> and oxidation and reduction peak currents and voltages were showed in the inset and the linearity was observed. The linearity of these curves indicates the facile charge transfer kinetics and the charge transfer process was diffusion controlled (Xiong et al., 2012) and these electrodes provide

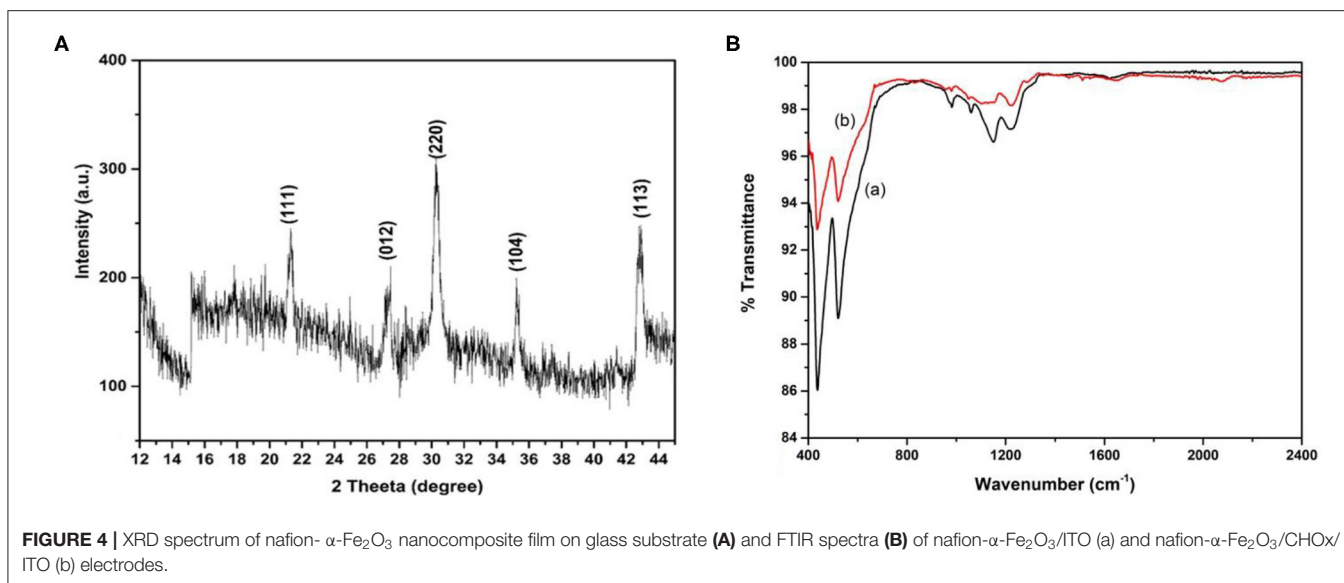


**FIGURE 4** | XRD spectrum of nafion-  $\alpha$ -Fe<sub>2</sub>O<sub>3</sub> nanocomposite film on glass substrate **(A)** and FTIR spectra **(B)** of nafion- $\alpha$ -Fe<sub>2</sub>O<sub>3</sub>/ITO (a) and nafion- $\alpha$ -Fe<sub>2</sub>O<sub>3</sub>/CHOx/ITO (b) electrodes.

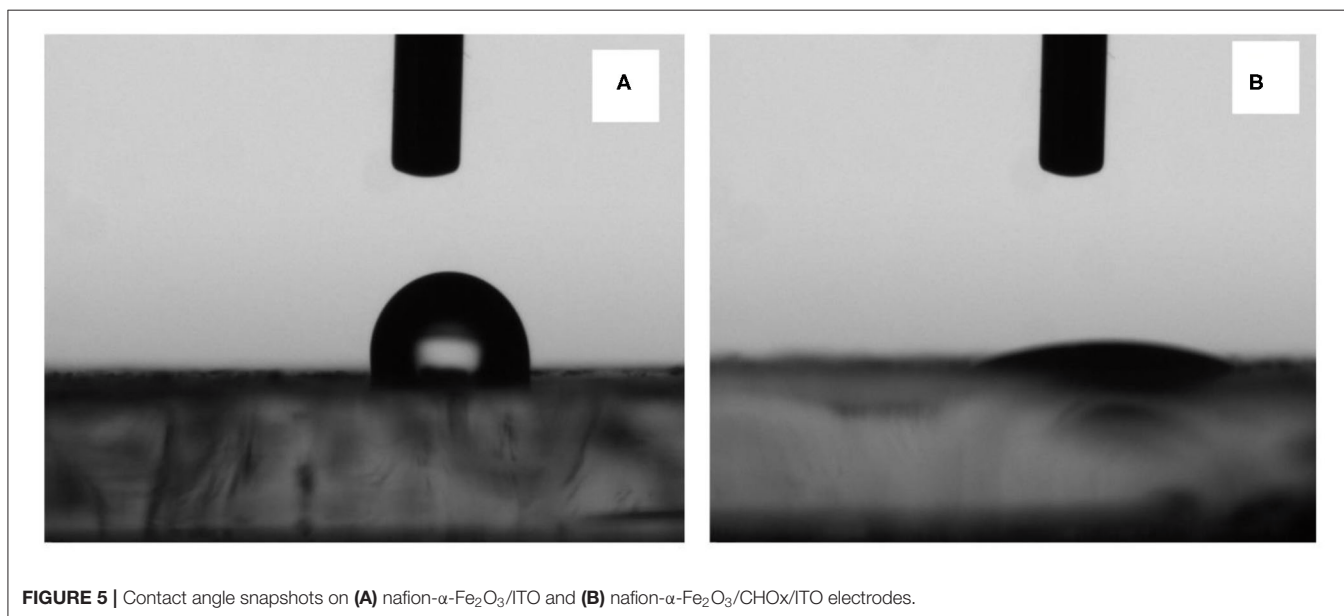


**FIGURE 5** | Contact angle snapshots on **(A)** nafion- $\alpha$ -Fe<sub>2</sub>O<sub>3</sub>/ITO and **(B)** nafion- $\alpha$ -Fe<sub>2</sub>O<sub>3</sub>/CHOx/ITO electrodes.

adequate conductivity for charge flow among electrode and electrolyte.

The different electrochemical parameters as  $E_a$ ,  $I_a$ ,  $E_c$ ,  $I_c$ , and the diffusion co-efficient ( $D$ ) of the Nafion- $\alpha$ -Fe<sub>2</sub>O<sub>3</sub>/ITO and Nafion- $\alpha$ -Fe<sub>2</sub>O<sub>3</sub>/CHOx/ITO electrodes found at the scan rate, 50 mV/s. The  $D$  value was assessed from the equation,

$$D = \frac{I_a^2}{(2.69 \times 10^5)^2 A^2 n^3 C^2 v} \quad (1)$$

where  $C$ ; the concentration of mediator buffer,  $A$ ; the area of the working electrode,  $n$ ; the number of electrons participated in redox process and  $v$ ; the scan rate.

The surface concentration ( $\gamma^*$ ) of the ionic species of the Nafion- $\alpha$ -Fe<sub>2</sub>O<sub>3</sub>/ITO and Nafion- $\alpha$ -Fe<sub>2</sub>O<sub>3</sub>/CHOx/ITO electrodes were assessed by Brown-Anson model (Bard and Faulkner, 2001) using the equation given by

$$\gamma^* = \frac{4RTI_a}{n^2 F^2 Av} \quad (2)$$

The values of the heterogeneous electron transfer rate constant ( $k_s$ ) was found for bioelectrodes using Laviron's equation (Singh et al., 2013).

$$k_s = \frac{mnFv}{RT} \quad (3)$$

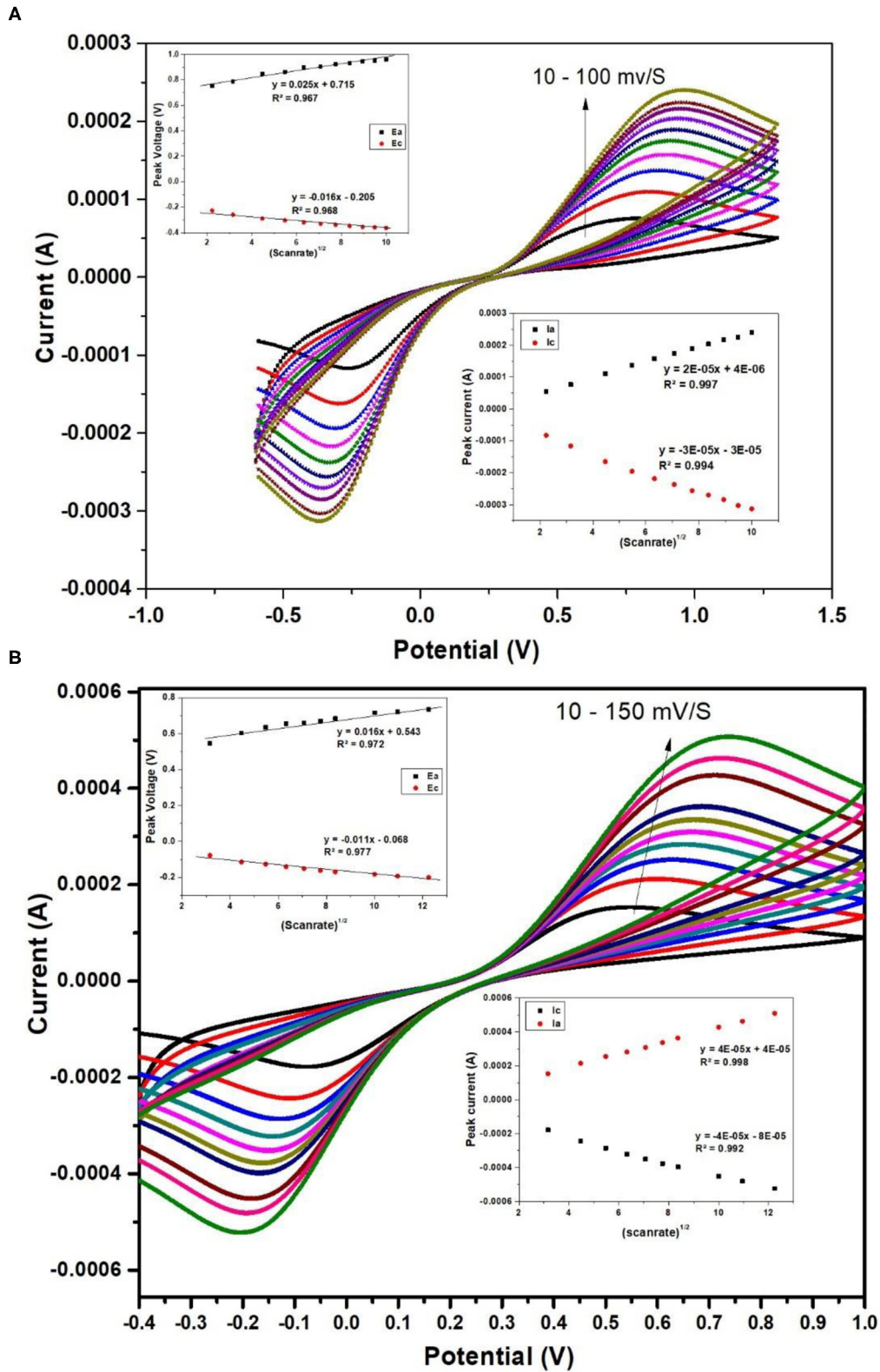


FIGURE 6 | CV curves of nafion- $\alpha$ -Fe<sub>2</sub>O<sub>3</sub>/ITO (A) and nafion- $\alpha$ -Fe<sub>2</sub>O<sub>3</sub>/CHOx/ITO (B) electrodes at different scan rates.

**TABLE 1** | Electrochemical parameters of Nafion-Fe<sub>2</sub>O<sub>3</sub>/ITO and Nafion-Fe<sub>2</sub>O<sub>3</sub>/CHOx/ITO electrodes.

| Electrode                                    | A (cm <sup>2</sup> )   | k <sub>s</sub> (s <sup>-1</sup> ) | γ*(mol/cm <sup>2</sup> ) | D (cm <sup>2</sup> s <sup>-1</sup> ) |
|--|------------------------|-----------------------------------|--------------------------|--------------------------------------|
| Fe <sub>2</sub> O <sub>3</sub> -naf/ITO      | 1.54 ( <i>r</i> = 0.7) | 1568.63                           | 4.288E-6                 | 8.954E-7                             |
| Fe <sub>2</sub> O <sub>3</sub> -naf-ChoX/ITO | 1.54 ( <i>r</i> = 0.7) | 421.55                            | 9.165E-6                 | 4.09E-6                              |

Where *m* is Δ*E* = *E*<sub>pa</sub> - *E*<sub>pc</sub>, *n* is the electrons participated in charge transfer, *F*; the Faraday constant, *v*; scan rate, *R*; the gas constant and *T*; room temperature.

The surface concentration of the redox species of electrodes was calculated using Brown–Anson model (Bard and Faulkner, 2001).

$$I_p = \frac{n^2 F^2 I^* A V}{4RT} \quad (4)$$

Where the slope of the scan rate vs. *I*<sub>pc</sub> is *I*<sub>p</sub>/*V* and the surface concentration of the electrode is *I*\*. All the electrochemical parameters are tabulated in **Table 1**.

## Electrochemical Response Studies

For cholesterol response measurements, nafion-α-Fe<sub>2</sub>O<sub>3</sub>/ITO and nafion-α-Fe<sub>2</sub>O<sub>3</sub>/CHOx/ ITO electrodes were positioned in the buffer and various concentrations of cholesterol solutions from 4 to 770 mg dl<sup>-1</sup> were added and DPV for each concentration was recorded. There is an increase in the peak current of Nafion-Fe<sub>2</sub>O<sub>3</sub>/ITO electrodes with increased concentrations was observed as shown in **Figure 7A**. The linear calibration plot of peak current with concentration was plotted and shown in inset of the **Figure 7A**.

The electrodes are suitable for sensing of cholesterol without any enzyme immobilization with sensitivity of 0.012 μA (mg/dl)<sup>-1</sup> cm<sup>-2</sup>. But, the crucial limitation of the enzyme less biosensor is the selectivity or specificity. The electrode was verified for selectivity with common interfering agents such as Ascorbic Acid (AA), Urea (U), 4-Acetymanophenol (4-AP), Citric Acid (CA), and glucose (Glu) at 4 mM concentrations and the results are shown in **Figure 8A**. Unfortunately, the Naf-Fe<sub>2</sub>O<sub>3</sub>/ITO electrode did not show much change in the peak currents as compared to cholesterol at 4 mM concentration implies the enzyme less sensing is not possible with real samples. Therefore, the enzyme cholesterol oxidase was immobilized on the electrode's surface by casting method through adsorption, dried, washed and dried again. The enzyme was immobilized without any cross-linking agent. The DPV response of different cholesterol concentrations on enzyme electrodes was tested. The DPV curves with different concentrations from a very low concentration from about 4–770 mg dl<sup>-1</sup> was carried out as given in **Figure 7B**. The peak currents vs. the concentration was plotted against and the obtained linearity plot was shown in the inset. The electrode sensitivity of was estimated as 64.93 × 10<sup>-2</sup> μA (mg/dl)<sup>-1</sup> cm<sup>-2</sup>. The enzyme-substrate interaction (Michaelis–Menten) constant *K*<sub>m</sub>, was obtained to

be 19 mg/dl. The lower detection limit (LOD) is obtained as 2 mg dl<sup>-1</sup>. The specificity or the selectivity was verified with the general interfering agents such as U, CA, 4-AP, AA, and glu at 4 mM concentrations, and the DPV peak currents of each of these analytes were less than the peak current of 4 mM cholesterol (**Figure 8B**) which confirmed the specificity of the developed electrode.

The synthesized nanocomposite was found suitable for the cholesterol sensing without the help of enzyme but without selectivity. Therefore, the enzymatic electrode was fabricated. The current values were found to increase after the enzyme immobilization with cholesterol concentration by showing the increase in the DPV peak current. The immobilization of CHOx on magnetic nanoparticles showed the improved biochemical activity and the immobilized CHOx proved to be the effective biocatalyst to catabolize cholesterol (Ghosh et al., 2018). The increased stability and activity of CHOx leading to the suitable application in biosensors (Ghosh et al., 2018). The enzyme mediated electrochemical reaction took place at the electrode surface (Nakaminami et al., 1997) causes the change in the current with the addition of cholesterol. The catabolic reaction of CHOx combined with the electrochemical oxidation of mediator at the surface of the electrode produces reduced CHOx [CHOx (red)] and cholestenon when cholesterol was added in the first step. When CHOx (red) was combined with the mediator (M) (ferri/ferro) at oxidation potential it produces CHOx (ox) and *M*<sub>red</sub> in the second step. In the third step, *M*<sub>red</sub> becomes again *M*<sub>ox</sub> by releasing electrons. The first and second steps utilize O<sub>2</sub>/H<sub>2</sub>O<sub>2</sub> which is available in the buffer solution and forms an intermediate in the reaction. The H<sub>2</sub>O<sub>2</sub> produced during second step gets electrochemically oxidize by giving the anodic current, which is the final measure of the cholesterol concentration. The schematic representation of the developed biosensing platform is given in **Figure 9**. The enzyme electrodes were found stable for almost 8 weeks when stored in the refrigerator, and after that the peak current started decreasing as shown in **Figure 10**.

## CONCLUSIONS

The present study represents the development of a selective enzymatic sensing platform for the detection of cholesterol. The sensing platform was based on the nanocomposite of iron oxide nanoparticles and the ionic conducting polymer nafion coated on the ITO coated glass substrate. The detection of cholesterol was carried out using electrochemical DPV method. The enzymatic sensor showed the better detection capability by showing higher sensitivity [64.93 × 10<sup>-2</sup> μA (mg/dl)<sup>-1</sup> cm<sup>-2</sup>] with better selectivity. The interaction of CHOx with cholesterol produced charge carriers which led to the increase in the DPV peak current with increased concentration. The semiconducting iron oxide nanoparticles helped in the transfer of electrons.



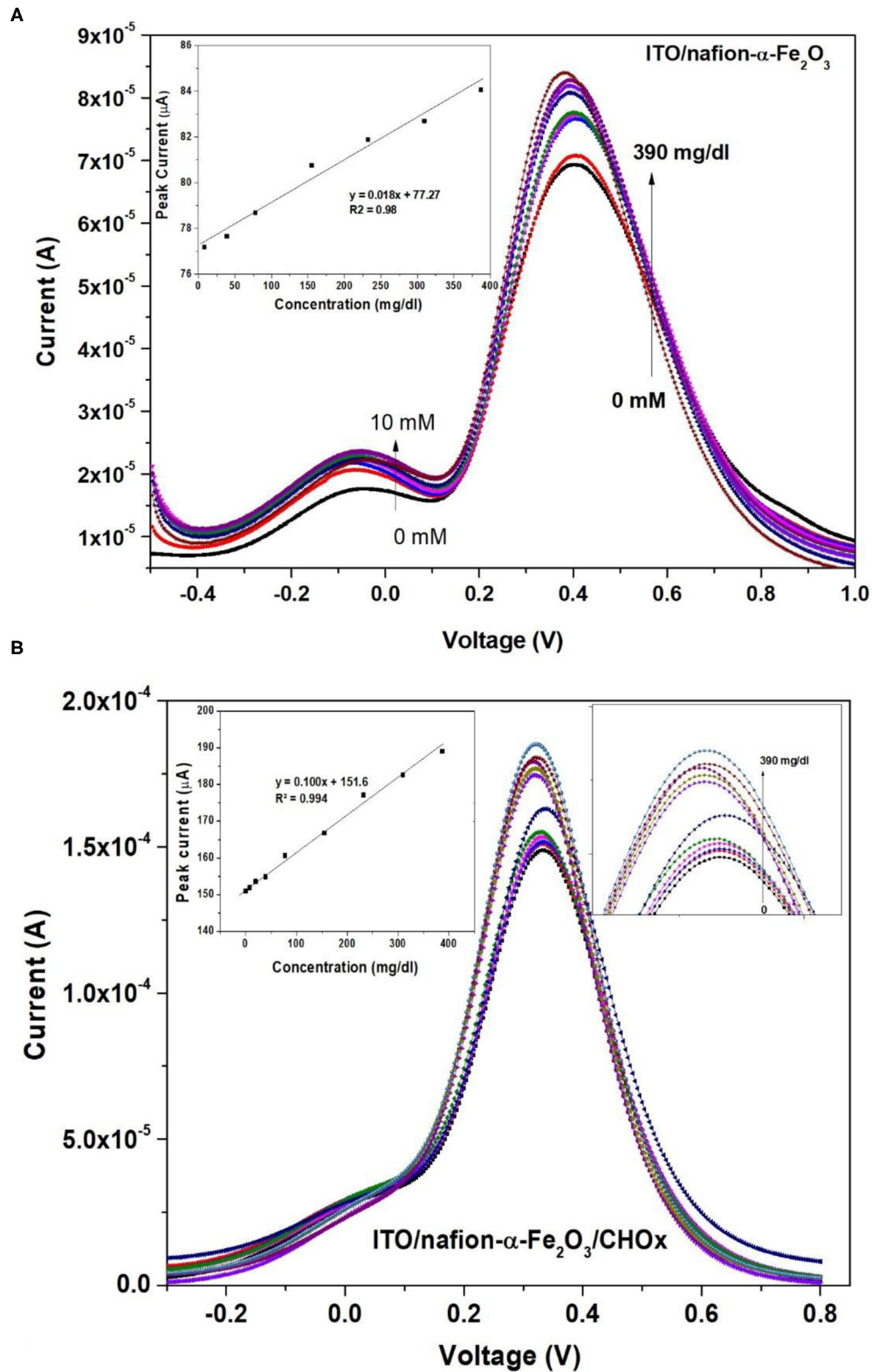


**FIGURE 7** | DPV of (A) nafion- $\alpha$ -Fe<sub>2</sub>O<sub>3</sub>/ITO (inset shows the calibration curve) and (B) nafion- $\alpha$ -Fe<sub>2</sub>O<sub>3</sub>/CHOx/ITO electrodes at different concentrations (insets show the calibration curve and enlarged peaks).

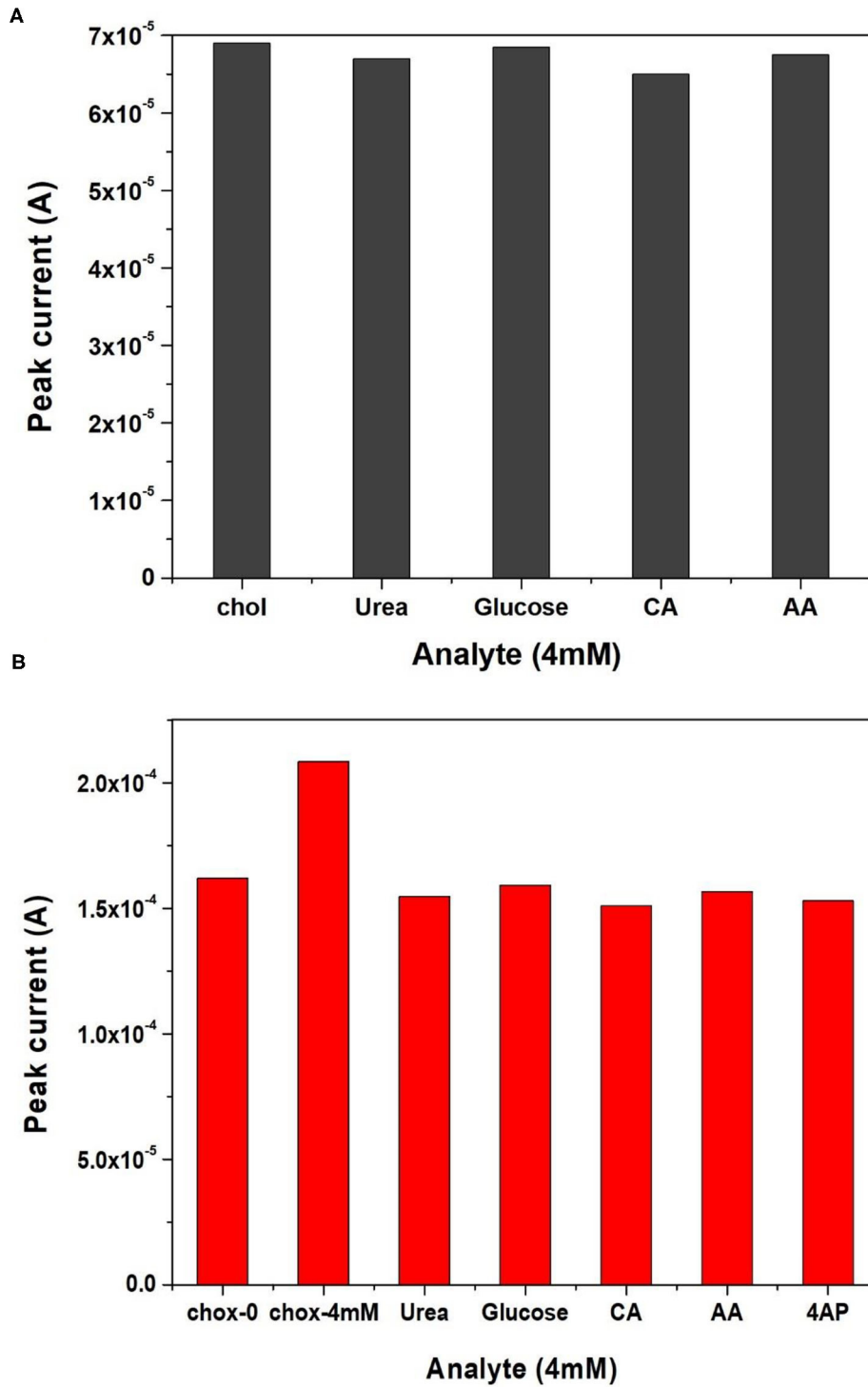


**FIGURE 8** | Selectivity studies of (A) nafion-Fe<sub>2</sub>O<sub>3</sub>/ITO and (B) nafion-Fe<sub>2</sub>O<sub>3</sub>/CHOx/ITO electrodes with different analytes.

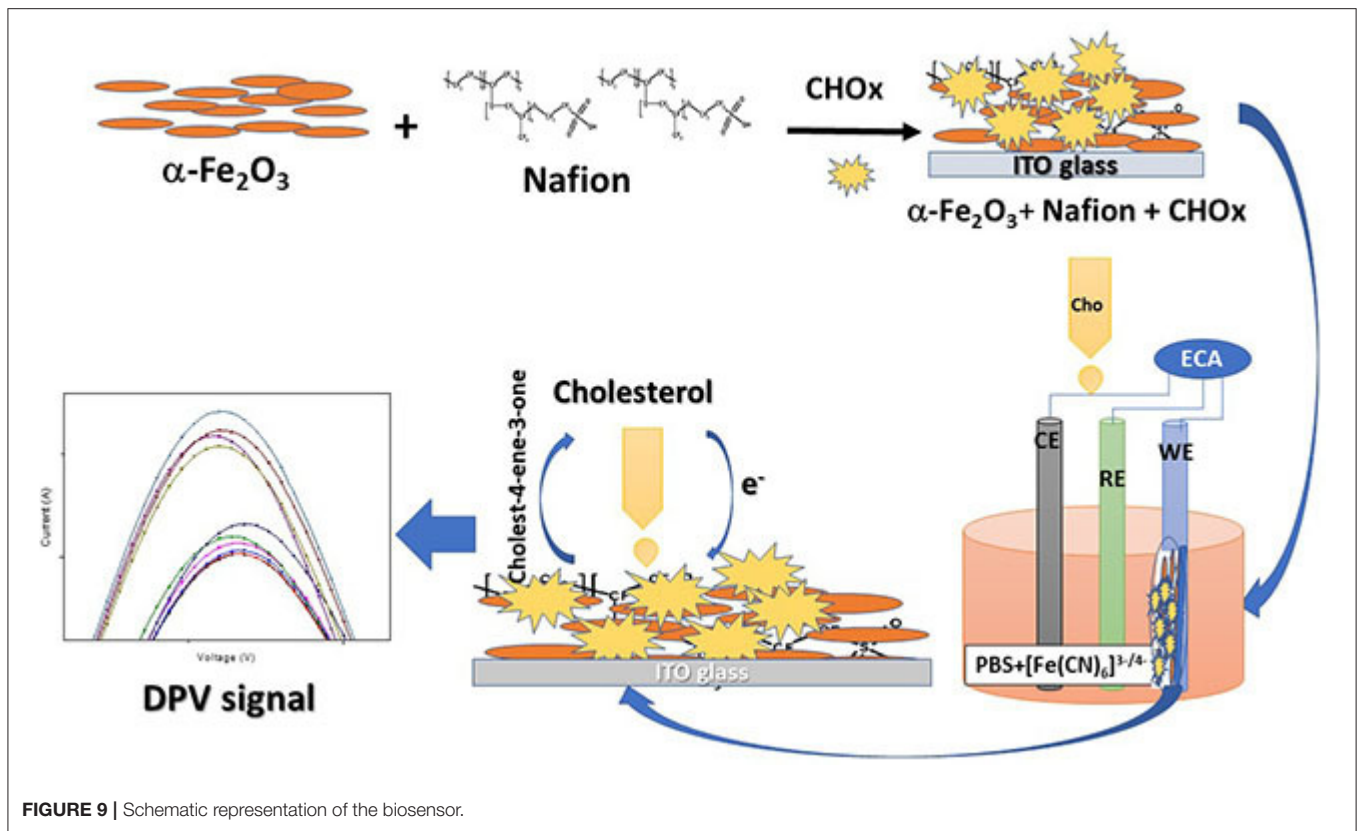


FIGURE 9 | Schematic representation of the biosensor.

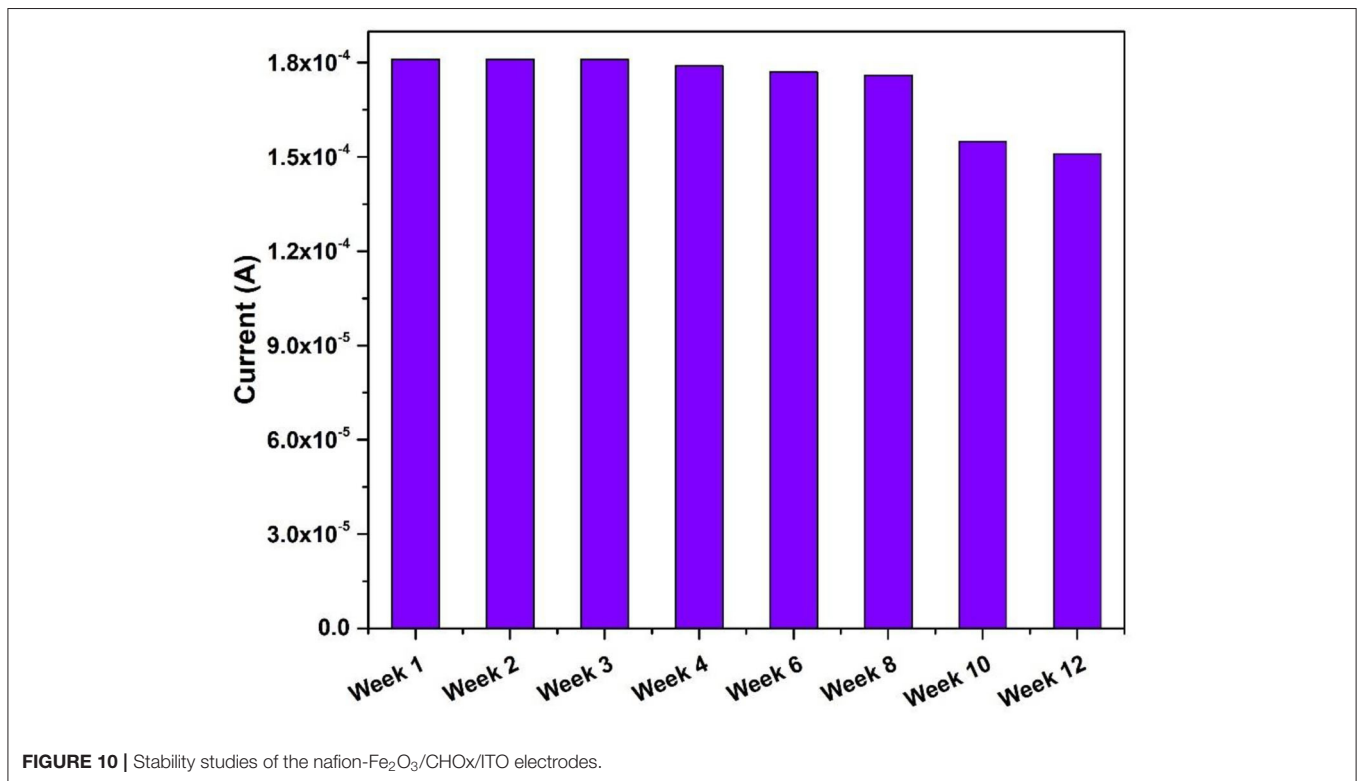


FIGURE 10 | Stability studies of the nafion- $\text{Fe}_2\text{O}_3/\text{CHOx}/\text{ITO}$  electrodes.

## DATA AVAILABILITY STATEMENT

The original contributions presented in the study are included in the article/supplementary material, further inquiries can be directed to the corresponding author/s.

## AUTHOR CONTRIBUTIONS

GL has formulated the study. IS and RP have carried out sample preparation and characterization part. All

authors participated in electrochemical characterization and sensing study.

## ACKNOWLEDGMENTS

GL was thankful to DST for funding through DST Women Scientist Project (SR/WOS-A/PM-108/2016). Dr. S. A. Khan was acknowledged for the SEM-EDS measurements.

## REFERENCES

- Ajayan, P. M., Schadler, L. S., and Braun, P. V. (2006). *Nanocomposite Science and Technology*. New York, NY: John Wiley and Sons. doi: 10.1002/3527602127
- Banerjee, A., Patra, S., Chakrabarti, M., Sanyal, D., Pal, M., and Pradhan, S. K. (2011). *Microstructure, Mössbauer, and Optical Characterizations of Nanocrystalline  $\alpha$ -Fe<sub>2</sub>O<sub>3</sub> Synthesized by Chemical Route*. Egypt: ISRN Ceramics.
- Bard, A. J., and Faulkner, L. R. (2001). Fundamentals and applications. *Electrochem. Methods* 2, 580–632.
- Bico, J., Thiele, U., and Quéré, D. (2002). Wetting of textured surfaces. *Colloids Surf. A Physicochem. Eng. Asp.* 206, 41–46. doi: 10.1016/S0927-7757(02)00061-4
- Chen, Y., Xin, Y., Yang, H., Zhang, L., Zhang, Y., Xia, X., et al. (2013). Immobilization and stabilization of cholesterol oxidase on modified sepharose particles. *Int. J. Biol. Macromol.* 56, 6–13. doi: 10.1016/j.ijbiomac.2013.01.026
- Chen, Y., Zhong, Q., Li, G., Tian, T., Tan, J., and Pan, M. (2018). Electrochemical study of temperature and Nafion effects on interface property for oxygen reduction reaction. *Ionics* 24, 3905–3914. doi: 10.1007/s11581-018-2533-3
- Demir, V., Ates, M., Arslan, Z., Camas, M., Celik, F., Bogatu, C., et al. (2015). Influence of Alpha and gamma-iron oxide nanoparticles on marine microalgae species. *Bull. Environ. Contam. Toxicol.* 95, 752–757. doi: 10.1007/s00128-015-1633-2
- Din, S. H. (2019). Nano-composites and their applications: a review. *Character. Appl. Nanomater.* 25, 407–415. doi: 10.24294/can.v2i1.875
- Ge, F., Li, M.-M., Ye, H., and Zhao, B.-X. (2012). Effective removal of heavy metal ions Cd<sup>2+</sup>, Zn<sup>2+</sup>, Pb<sup>2+</sup>, Cu<sup>2+</sup> from aqueous solution by polymer-modified magnetic nanoparticles. *J. Hazard. Mater.* 211, 366–372. doi: 10.1016/j.jhazmat.2011.12.013
- Ghosh, S., Ahmad, R., Gautam, V. K., and Khare, S. K. (2018). Cholesterol-oxidase-magnetic nanobioconjugates for the production of 4-cholesten-3-one and 4-cholesten-3, 7-dione. *Bioresour. Technol.* 254, 91–96. doi: 10.1016/j.biortech.2018.01.030
- Gonzalez, C. M., Hernandez, J., Peralta-Videa, J. R., Botez, C. E., Parsons, J. G., and Gardea-Torresdey, J. L. (2012). Sorption kinetic study of selenite and selenate onto a high- and low-pressure aged iron oxide nanomaterial. *J. Hazard. Mater.* 211, 138–145. doi: 10.1016/j.jhazmat.2011.08.023
- Grover, V. A., Hu, J., Engates, K. E., and Shipley, H. J. (2012). Adsorption and desorption of bivalent metals to hematite nanoparticles. *Environ. Toxicol. Chem.* 31, 86–92. doi: 10.1002/etc.712
- Hasanabadi, N., Ghaffarian, S. R., and Hasani-Sadrabadi, M. M. (2013). Nafion-based magnetically aligned nanocomposite proton exchange membranes for direct methanol fuel cells. *Solid State Ion.* 232, 58–67. doi: 10.1016/j.ssi.2012.11.015
- Jun, Y. W., Lee, J. H., and Cheon, J. (2008). Chemical design of nanoparticle probes for high-performance magnetic resonance imaging. *Angew. Chem. Int. Ed. Engl.* 47, 5122–5135. doi: 10.1002/anie.200701674
- Kaushik, A., Khan, R., Solanki, P. R., Pandey, P., Alam, J., Ahmad, S., et al. (2008a). Iron oxide nanoparticles–chitosan composite based glucose biosensor. *Biosens. Bioelectron.* 24, 676–683. doi: 10.1016/j.bios.2008.06.032
- Kaushik, A., Solanki, P. R., Ansari, A. A., Ahmad, S., and Malhotra, B. D. (2008b). Chitosan–iron oxide nanobiocomposite based immunosensor for ochratoxin-A. *Electrochem. Commun.* 10, 1364–1368. doi: 10.1016/j.elecom.2008.07.007
- Kaushik, A., Solanki, P. R., Ansari, A. A., Sumana, G., Ahmad, S., and Malhotra, B. D. (2009). Iron oxide-chitosan nanobiocomposite for urea sensor. *Sens. Actuators B Chem.* 138, 572–580. doi: 10.1016/j.snb.2009.02.005
- Kurihara, Y., Mabuchi, T., and Tokumasu, T. (2017). Molecular analysis of structural effect of ionomer on oxygen permeation properties in PEFC. *J. Electrochem. Soc.* 164:F628. doi: 10.1149/2.1301706jes
- Mallick, P., and Dash, B. N. (2013). X-ray diffraction and UV-visible characterizations of  $\alpha$ -Fe<sub>2</sub>O<sub>3</sub> nanoparticles annealed at different temperature. *J. Nanosci. Nanotechnol.* 3, 130–134. doi: 10.5923/j.nn.20130305.04
- Mehrotra, P. (2016). Biosensors and their applications—a review. *J. Oral Biol. Craniof. Res.* 6, 153–159. doi: 10.1016/j.jobcr.2015.12.002
- Nakaminami, T., Kuwabata, S., and Yoneyama, H. (1997). Electrochemical oxidation of cholesterol catalyzed by cholesterol oxidase with use of an artificial electron mediator. *Anal. Chem.* 69, 2367–2372. doi: 10.1021/ac960996p
- Paul, D. K., and Karan, K. (2014). Conductivity and wettability changes of ultrathin Nafion films subjected to thermal annealing and liquid water exposure. *J. Phys. Chem. C* 118, 1828–1835. doi: 10.1021/jp410510x
- Paul, D. K., Shim, H. K., Giorgi, J. B., and Karan, K. (2016). Thickness dependence of thermally induced changes in surface and bulk properties of Nafion nanofilms. *J. Polym. Sci. Part B Polymer Phys.* 54, 1267–1277. doi: 10.1002/polb.24034
- Perez, J. (2007). Iron oxide nanoparticles—Hidden talent. *Nat. Nanotech.* 2, 535–536. doi: 10.1038/nnano.2007.282
- Raymond, L., Revol, J. F., Ryan, D. H., and Marchessault, R. H. (1996). Precipitation of ferrites in Nafion membranes. *J. App. Poly. Sci.* 59, 1073–1086. doi: 10.1002/(SICI)1097-4628(19960214)59:7<1073::AID-APP4>3.0.CO;2-B
- Sharma, R., Agrawal, V. V., Srivastava, A. K., Nain, L., Imran, M., Kabi, S. R., et al. (2013). Phase control of nanostructured iron oxide for application to biosensor. *J. Mater. Chem. B* 1, 464–474. doi: 10.1039/C2TB00192F
- Singh, B., Ali, N., Chakravorty, A., Sulania, I., Ghosh, S., and Kabiraj, D. (2019). Wetting behavior of MoS<sub>2</sub> thin films. *Mater. Res. Express* 6:096424. doi: 10.1088/2053-1591/ab2e5a
- Singh, J., Roychoudhury, A., Srivastava, M., Solanki, P. R., Lee, D. W., Lee, S. H., et al. (2013). A highly efficient rare earth metal oxide nanorods based platform for aflatoxin detection. *J. Mater. Chem. B* 1, 4493–4503. doi: 10.1039/C3TB20690D
- Singh, U. B., Yadav, R. P., Pandey, R. K., Agarwal, D. C., Pannu, C., and Mittal, A. K. (2016). Insight mechanisms of surface structuring and wettability of ion-treated Ag thin films. *J. Phys. Chem. C* 120, 5755–5763. doi: 10.1021/acs.jpcc.5b11944
- Sulania, I., Kaswan, J., Attatappa, V., Karn, R. K., Agarwal, D. C., and Kanjilal, D. (2016). “Investigations of electrical and optical properties of low energy ion irradiated  $\alpha$ -Fe<sub>2</sub>O<sub>3</sub> (hematite) thin films,” in *AIP Conference Proceedings, Vol. 1731* (Indonesia: AIP Publishing LLC), 120021. doi: 10.1063/1.4948093
- Sulania, I., Yadav, R. P., and Karn, R. K. (2018). “Atomic and magnetic force studies of co thin films and nanoparticles: understanding the surface correlation using fractal studies,” in *Handbook of Materials Characterization*, ed S. Sharma (Cham: Springer), 263–291. doi: 10.1007/978-3-319-92955-2\_7



- Umar, A., Ahmad, R., Hwang, S. W., Kim, S. H., Al-Hajry, A., and Hahn, Y. B. (2014). Development of highly sensitive and selective cholesterol biosensor based on cholesterol oxidase co-immobilized with  $\alpha$ -Fe<sub>2</sub>O<sub>3</sub> micro-pine shaped hierarchical structures. *Electrochim. Acta* 135, 396–403. doi: 10.1016/j.electacta.2014.04.173
- Woo, K., Lee, H. J., Ahn, J. P., and Park, Y. S. (2003). Sol-gel mediated synthesis of Fe<sub>2</sub>O<sub>3</sub> nanorods. *Adv. Mater.* 15, 1761–1764. doi: 10.1002/adma.200305561
- Xiong, S., Yang, F., Jiang, H., Ma, J., and Lu, X. (2012). Covalently bonded polyaniline/fullerene hybrids with coral-like morphology for high-performance supercapacitor. *Electrochim. Acta* 85, 235–242. doi: 10.1016/j.electacta.2012.08.056

**Conflict of Interest:** The authors declare that the research was conducted in the absence of any commercial or financial relationships that could be construed as a potential conflict of interest.

Copyright © 2020 Sulania, Pricilla and Lakshmi. This is an open-access article distributed under the terms of the Creative Commons Attribution License (CC BY). The use, distribution or reproduction in other forums is permitted, provided the original author(s) and the copyright owner(s) are credited and that the original publication in this journal is cited, in accordance with accepted academic practice. No use, distribution or reproduction is permitted which does not comply with these terms.